FPC AND HI-PASS FILTER HOM COUPLER DESIGN FOR THE RF DIPOLE CRAB CAVITY FOR THE LHC HILUMI UPGRADE*

Zenghai Li[1], SLAC, Menlo Park, CA 94025, USA
J. R. Delayen, S. U. De Silva, HyeKyoung Park, and R. G. Olave, ODU, Norfolk, VA 23529, USA

Abstract

A 400-MHz compact RF dipole (RFD) crab cavity design was jointly developed by Old Dominion University and SLAC under the support of US LARP program for the LHC HiLumi upgrade. The RFD cavity design is consisted of a rounded-square tank and two ridged deflecting poles, operating with a TE11-like dipole mode, which is the lowest mode of the cavity. A prototype RFD cavity is being manufactured and will be tested on the SPS beam line at CERN. The coaxial fundamental Power Coupler (FPC) of the prototype cavity was re-optimized to minimizing the power heating on the coupler internal antenna. A hi-pass filter HOM damping coupler was developed to achieve the required wakefield damping while maintaining a compact size to fit into the beam line space. In this paper, we will discuss the details of the RF optimization and tolerance analyses of the FPC and HOM couplers.

INTRODUCTION

A crabbing scheme [1] has been adopted as the baseline tool for the LHC HiLumi upgrade. The nominal scheme for the HL-LHC is the local crabbing with the 400 MHz superconducting deflecting cavities. Due to the small beam line separation close to the IP, the transverse size of the crab cavity is limited to 145-mm. To meet such a space constraint, an RF dipole (RFD) cavity [2-6] is being developed by a SLAC and ODU joint effort. The RFD design in concern is shown in Fig. 1. It consists of a rounded-square tank and two ridged deflecting poles. The operating mode is a TE11-like dipole mode, which is the fundamental mode. The frequency of the TE11-like mode is in principle not constrained by the cavity dimension in the deflecting plane, so the cavity dimension can be very compact. The rounded-square shape chosen for the present design is to accommodate for both the horizontal and vertical crabbing schemes. The present design also incorporates a curved pole profile as shown in Fig. 1 to improve the field uniformity within the beam aperture. Table 1 lists the major dimensions and RF parameters of the cavity. The lowest HOM frequency is more than 230 MHz above the operating mode. This large mode separation provides flexibilities of implementing different damping schemes for the HOMs using either waveguide [5] or high-pass filter HOM couplers. In this paper, we present a newly developed high-pass filter HOM coupler and the optimized FPC coupler design for the RFD cavity. This cavity design is being manufactured and will be tested on the SPS at CERN [7,8].

* This work was supported by DOE Contract No. DE-AC02-76SF00515 and was partially supported by the DOE through the US LHC Accelerator Research Program (LARP). Computations used computer resources at NERSC, LBNL.
[1]lizh@slac.stanford.edu

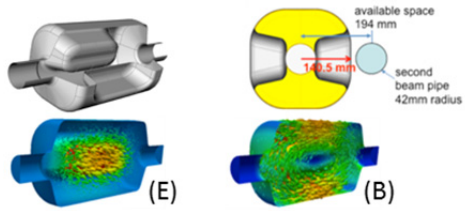

Figure 1: RFD crab cavity and the field patterns.

Table 1: RFD Crab Cavity RF Parameters

Frequency (MHz)	400
Operating Mode	TE11
Lowest dipole HOM (MHz)	634
Lowest acc HOM (MHz)	715
Iris aperture (diameter) (mm)	84
Transverse dimension (mm)	281x281
Longitudinal dimension (w/o couplers) (mm)	556
R_T (ohm/cavity)	433
V_T (MV/cavity)	3.34
Bs (mT)	55.6
Es (MV/m)	33.4

HOM COUPLERS

The HOM mode spectrum calculated using Omega3P [9,10] up to 2 GHz is shown in Fig. 2. The first HOM is a horizontal dipole mode at 634 MHz. The first important accelerating mode is at 761 MHz and the first vertical dipole mode is at 783 MHz.

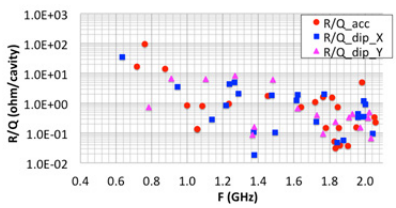

$$\left(\frac{R}{Q}\right)_L = \frac{1}{2}\frac{|V_\perp|^2}{\omega U}$$

$$\left(\frac{R}{Q}\right)_T = \frac{1}{2}\frac{|V_\perp(r_0)|^2}{\omega U\left(\frac{\omega}{c}r_0\right)^2}$$

Figure 2: HOM mode spectrum.

The HOM and FPC coupler design were to meet the following design requirements: 1) be clear of the second beam line which is 194 mm away; 2) all coupler ports are oriented in the up-vertical direction to simplify the cryostat design; 3) the HOM couplers need be able to handle high HOM power that could potentially be generated by the beam. For example, the maximum beam (σ_z=76 mm) induced power by the first major accelerating mode at 761 MHz (R/Q~200) is $48 I_b^2 Q_{ext}$. A half-ampere beam would produce a power of 3.6 kW for a Q_{ext} of 300

if the beam is on resonance. Thus a lower Q_{ext} is desirable even if beam breakup can tolerate a higher Q_{ext}. Two HOM couplers are needed, one for the horizontal HOMs and one for the vertical HOMs. Both contribute to the damping of the accelerating HOMs.

Horizontal HOM Coupler (deflecting plane)

The horizontal HOM coupler needs to reject the operating mode while providing effective coupling to the horizontal HOMs. The coupler is consisted of a waveguide stub that connects to the cavity at the end-plate and a high-pass filter circuit as shown in Fig. 3. The operating mode in the RFD has low surface fields at the end-plate by design so the slot opening to the HOM coupler does not cause any high field enhancement. The waveguide stub has a higher cut off frequency and induces attenuation of the operating modes fields to the filter circuit, which minimizes the RF heating on the high-pass filter. The coupling of the coupler to the HOMs is through the magnetic field. Both the horizontal HOMs and the accelerating HOMs can be damped via this coupler. Simulation has shown that one such coupler is sufficient to provide the required damping. To maintain the field symmetry, a symmetrizing stub is attached on the opposite side, which is later used as the FPC port.

Fig. 3 shows the high-pass filter geometry and the pass-band transmission. A better than -5dB transmission is achieved at frequencies above 600MHz. The rejection at the 400 MHz is about -60dB by the filter. The field contour plot in figure 3 is at 400 MHz to show the rejection of the operating mode.

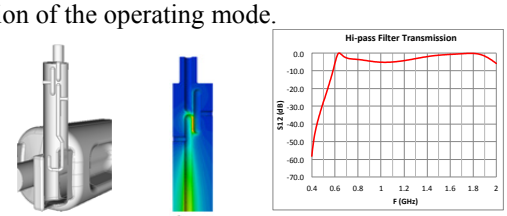

Figure 3: High-pass filter HOM coupler.

Vertical HOM Coupler

The vertical HOM coupler consists of a waveguide stub and a coaxial pickup located at the center plane as shown in Fig. 4. Due to polarity and symmetry of the operating mode, both the waveguide stub and the coaxial pickup naturally reject coupling to the operating mode. Thus no filter is needed. This coupler also couples to the accelerating HOMs. A small offset (7 mm) is incorporated into the pickup tip to enhance coupling to the dipole modes at around 2 GHz, at a small cost of a ~1.5 W RF power leakage through the coupler.

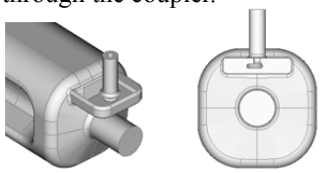

Figure 4: Selective coupler for the vertical HOM.

HOM Damping Results

The Q_{ext} calculated using Omega3P for modes up to 2 GHz is plotted in Fig. 5 (left). The impedances of the HOMs ($(R/Q)*Q_{ext}$) are plotted in Fig. 5 (right). The solid lines are the impedance budget for dipole HOMs (blue) and accelerating HOMs (red) respectively. All modes are within the impedance requirement.

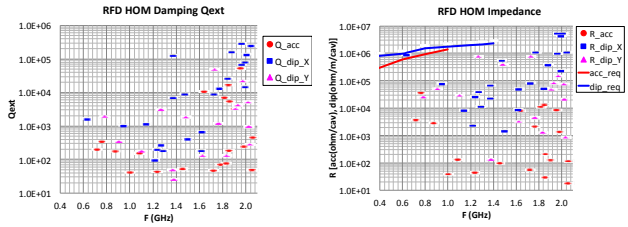

Figure 5: The Q_{ext} and impedance of the HOMs.

HIGH-PASS FILTER TOLERANCES

The performance of the high-pass filter HOM coupler relies on a good broadband transmission at the HOM frequencies, and a nearly zero transmission at the operating mode frequency. It is essential the design to have acceptable tolerances on dimension errors. We evaluated the filter transmission and rejection properties by offsetting the coupler dimensions comparable to machine tolerance specifications as indicated in Fig. 6(a). The most sensitive region of the transmission to the dimension errors is in the rise region from 0.4-0.6 GHz, which may affect the rejection of the operating mode. The worse effect among the cases calculated is a 0.27 W leakage of RF power. There is no significant degradation of transmission within the pass-band from 0.6 to 2 GHz. None of these dimension errors cause a significant deterioration in the HOM Q_{ext}, Fig. 6(b). More detailed RFD cavity tolerance studies are presented in [11].

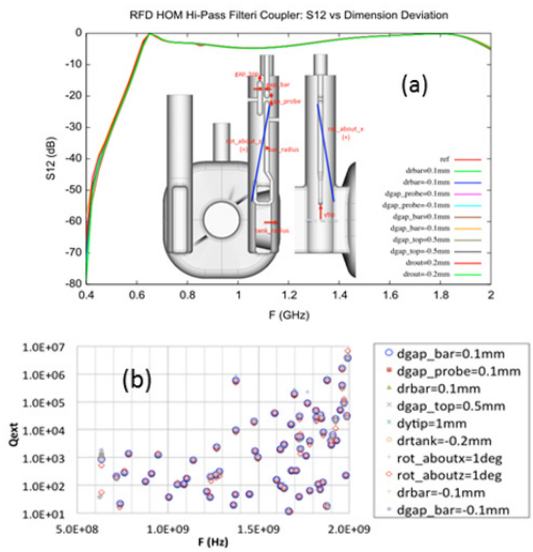

Figure 6. Sensitivity of Q_{ext} on coupler dimension errors.

FPC COUPLER

The symmetrising stub opposite to the horizontal HOM coupler is used as the power coupling port as shown in Fig. 7. The waveguide stub is adapted to a coaxial coupler that has an inner conductor diameter of 27 mm and outer conductor diameter of 62 mm. The hook shaped probe is optimized to enhance the coupling so that the hook does not need to be inserted into the higher field

ISBN 978-3-95450-168-7

region to achieve the required coupling ($5x10^5$), effectively reducing the RF heating on the copper gasket.

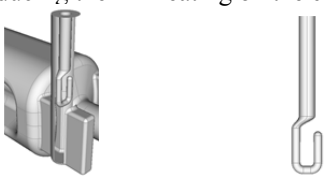

Figure 7: FPC coupler and hook antenna.

RF AND HOM HEATING ON COUPLER

RF heating: The RF heating on the various coupler surfaces was evaluated for the thermal engineering design. Figure 8 shows the values at the 3.4 MV deflecting voltage. The H-hook and H-T are made of niobium and assumed a 10 nΩ R_S at 2 K. The H-probe, V-probe and the HHOM Cu gasket are made of copper and assumed a 1 mΩ R_S at 2 K. The FPC-hook is made of copper and assumed a 5 mΩ R_S (copper value at room temperature). The RF heating on the FPC hook is 67.5 W and is below the specification of 70 W.

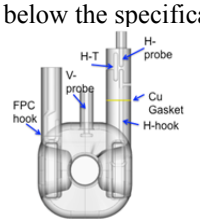

Coupler part	RF Heating (W)	
fpc-hook	6.75E+01	
HHOM Cu gasket	1.07E-01	2K
H-hook	5.99E-04	2K
H-T	1.44E-06	2K
H probe	4.90E-02	2K
V-probe	9.32E-02	2K

Figure 8: RF heating due to operating mode.

HOM heating: The beam induced HOM power may cause HOM heating on the coupler. The HOM heating was estimated by assuming a 1 kW power for each HOM mode propagating through the coupler (this is based on the assumption of beam close to resonance). The heating obtained with this assumption is less than 7 micro-W on the Nb surfaces, less than 0.1 W on the Cu probes, and less than 1 mW on the Cu gasket.

The RF and HOM heating on the HOM coupler was validated via thermal analysis and is well within the design limitations [8].

MP IN THE HOM AND FPC COUPLERS

Multipacting (MP) analyses were carried out using Track3P [12]. The field level was scanned up to 6 MV of deflecting voltage with a 0.25 MV interval. Resonant trajectories were searched at each field level. The impact energy of the resonant particles was obtained. The SEY of the Nb and Cu is used as an indication of potential strength of the MP. Typical SEY curves for Nb and Cu are shown in Fig. 9. The max SEY for Nb is at around 300 eV, and is at around 700 eV for Cu.

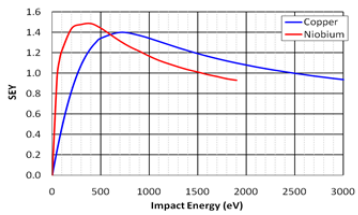

Figure 9: SEY dependence on impact energy for niobium and copper.

MP in the High-pass Filter HOM Coupler

There was no significant MP band in the high-pass filter. A narrow MP band in the coupling gap existed if the gap is flat as shown in Figure 10. The tips were fully rounded in the final design, which effectively eliminated the MP band in the coupler.

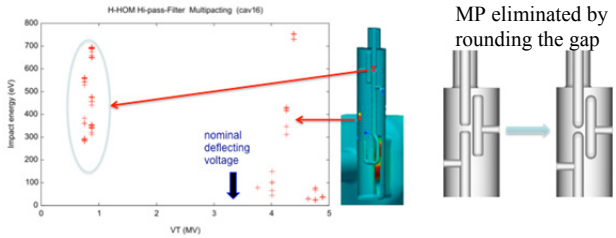

Figure 10: MP band in the high-pass filter HOM coupler. The MP band was eliminated by rounding the gap.

MP in the FPC Coupler

There were no significant MP trajectories found in the region of the waveguide stub. There is a MP band in the hook region at low deflecting voltages. It is of the two-point type between the Nb and Cu surfaces. The impact energy on the Cu hook surface is below 350 eV. This band is not expected to be a hard barrier. The MP band above the 4 MV deflecting voltage is located in the regular coax region. It is also a two-point type between the Nb and Cu surfaces. The impact energy on the outer Nb surface is over 1700 eV. The SEY for Nb is low at these energies.

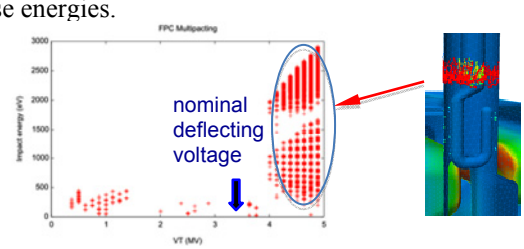

Figure 11: MP in the FPC coupler.

MP in the Vertical HOM Coupler

There is no MP trajectories found in the vertical HOM coupler region because the coupler does not couple to the deflecting mode. There is virtually no field in the coupler.

SUMMARY

The FPC and a high-pass filter HOM coupler were developed and optimized for the RFD crab cavity. The tolerances on the filter are acceptable and feasible for manufacturing. The RF heating on the coupler is low and posts no issues for the engineering design. Multipacting simulations reveal no significant issues in the couplers. The design is being manufactured and will be tested on the SPS.

The authors would like to acknowledge helpful discussions of the LHC/LARP crab cavity collaboration colleagues in the LHC/LARP crab cavity meetings.

REFERENCES

[1] https://twiki.cern.ch/twiki/bin/view/Main/LHCCrabCavities.

[2] Zenghai Li and Lixin Ge, “Compact Crab Cavity for H and V Crabbing,” US LARP Collaboration Meeting, Montauk, NY, May 2011.
[3] J. R. Delayen and S. U. de Silva, “ODU/JLAB Parallel-Bar Cavity Development,” US LARP Collaboration Meeting, Montauk, NY, May 2011.
[4] Zenghai Li, et al., “RF Modeling Using Parallel Codes ACE3P for the 400-MHz Parallel-bar/Ridged-waveguide Compact Crab Cavity for the LHC HiLumi Upgrade,” Proc. IPAC2012, New Orleans.
[5] Zenghai Li, et al., „Hom Damping Coupler Design For The 400-Mhz Rf Dipole Compact Crab Cavity For The Lhc Hilumi Upgrade,” Proc. IPAC2013, Shanghai, China.
[6] S. U. De Silva, et al, “Proof-of-Principle cavity preparation and testing, RFD cavity”, Proc. IPAC2013, Shanghai, China.
[7] S. U. De Silva, et al., “Design and Prototyping of a 400 MHz RF-Dipole Crabbing Cavity for the LHC High-Luminosity Upgrade”, in This Proceedings of IPAC 2015, Richmond, VA, USA, 2015.
[8] H. Park et al., “Engineering Study of Crab Cavity HOM Couplers for LHC High Luminosity Upgrade”, in This Proceedings of IPAC 2015, Richmond, VA, USA, 2015.
[9] K. Ko, et al., “Advances in Parallel Computing Codes for Accelerator Science and Development,” Proc. LINAC2010, Tsukuba, Japan, 2010.
[10] Lie-Quan Lee, et al., Omega3P: A Parallel Finite-Element Eigenmode Analysis Code for Accelerator Cavities, SLAC-PUB-13529, 2009.
[11] S. U. De Silva, et al., “Imperfection and Tolerance Analysis of HOM Couplers for LHC High-Luminosity Upgrade”, in This Proceedings of IPAC 2015, Richmond, VA, USA, 2015.
[12] L. Ge, et al., "Multipacting Simulations of TTF-III Power Coupler Components," Proc. PAC07, Albuquerque, New Mexico.

ISBN 978-3-95450-168-7